# NAVAL POSTGRADUATE SCHOOL
## Monterey, California

AD-A245 950

# THESIS

ANALYSIS OF THE EFFECTS OF IONOSPHERIC
SAMPLING OF REFLECTION POINTS NEAR-PATH, FOR
HIGH-FREQUENCY SINGLE-SITE-LOCATION DIRECTION
FINDING SYSTEMS

by

Carlos Augusto Teixeira Filho

December, 1990

Thesis Advisor:                                    Richard W. Adler

Approved for public release; distribution is unlimited.

92-03480

# REPORT DOCUMENTATION PAGE

Form Approved
OMB No. 0704-0188

| 1a. REPORT SECURITY CLASSIFICATION UNCLASSIFIED | 1b. RESTRICTIVE MARKINGS |
|---|---|
| 2a. SECURITY CLASSIFICATION AUTHORITY | 3. DISTRIBUTION / AVAILABILITY OF REPORT |
| 2b. DECLASSIFICATION / DOWNGRADING SCHEDULE | Approved for public release; distribution is unlimited |

| 4. PERFORMING ORGANIZATION REPORT NUMBER(S) | 5. MONITORING ORGANIZATION REPORT NUMBER(S) |
|---|---|

| 6a. NAME OF PERFORMING ORGANIZATION NAVAL POSTGRADUATE SCHOOL | 6b. OFFICE SYMBOL (If applicable) 3A | 7a. NAME OF MONITORING ORGANIZATION NAVAL POSTGRADUATE SCHOOL |
|---|---|---|

| 6c. ADDRESS (City, State, and ZIP Code) Monterey, CA 93943-5000 | 7b. ADDRESS (City, State, and ZIP Code) Monterey, CA 93943-5000 |
|---|---|

| 8a. NAME OF FUNDING / SPONSORING ORGANIZATION | 8b. OFFICE SYMBOL (If applicable) | 9. PROCUREMENT INSTRUMENT IDENTIFICATION NUMBER |
|---|---|---|

| 8c. ADDRESS (City, State, and ZIP Code) | 10. SOURCE OF FUNDING NUMBERS | | | |
|---|---|---|---|---|
| | PROGRAM ELEMENT NO. | PROJECT NO. | TASK NO. | WORK UNIT ACCESSION NO. |

11. TITLE (Include Security Classification)
ANALYSIS OF THE EFFECTS OF IONOSPHERIC SAMPLING OF REFLECTION POINTS NEAR-PATH, FOR HIGH-FREQUENCY SINGLE-SITE-LOCATION DIRECTION FINDING SYSTEMS

12. PERSONAL AUTHOR(S)
Teixeira Filho, Carlos A.

| 13a. TYPE OF REPORT Master's Thesis | 13b. TIME COVERED FROM _____ TO _____ | 14. DATE OF REPORT (Year, Month, Day) December 1990 | 15. PAGE COUNT 67 |
|---|---|---|---|

16 SUPPLEMENTARY NOTATION
The views expressed in this thesis are those of the author and do not reflect the official policy or position of the Department of Defense of the U.S. Govt

| 17. COSATI CODES | | | 18. SUBJECT TERMS (Continue on reverse if necessary and identify by block number) |
|---|---|---|---|
| FIELD | GROUP | SUB-GROUP | Single-Site-Location, Direction-Finding, High-Frequency, Estimation, Sampling |
| | | | |

19 ABSTRACT (Continue on reverse if necessary and identify by block number)
This thesis suggests a method to estimate the current value of an ionospheric parameter. The proposed method is based on the known variability of the observed current values near path and utilizes data derived from ionospheric sampling measurements. Analysis of errors is provided in Single-Site-Location High-Frequency Direction Finding (SSL-HFDF), arising from ionospheric irregularities such as Es (sporadic E), ionospheric tilts, and traveling ionospheric disturbances (TIDs). The characteristics of Es, tilts and TIDs for mid-latitudes are summarized in tables. The spatial and temporal coherence of ionospheric variabilities and irregularities is analyzed over the electron density. Practical results, measurements, and studies are presented on SSL-HFDF. A survey of characteristics of the ionosphere in the equatorial region is also provided. Finally, some recommendations are given to maximize the applicability of the proposed method.

| 20 DISTRIBUTION / AVAILABILITY OF ABSTRACT ☑ UNCLASSIFIED/UNLIMITED ☐ SAME AS RPT ☐ DTIC USERS | 21. ABSTRACT SECURITY CLASSIFICATION UNCLASSIFIED | |
|---|---|---|
| 22a. NAME OF RESPONSIBLE INDIVIDUAL Richard W. Adler | 22b TELEPHONE (Include Area Code) (408)6462352 | 22c OFFICE SYMBOL EC/Ab |

DD Form 1473, JUN 86          Previous editions are obsolete.          SECURITY CLASSIFICATION OF THIS PAGE

S/N 0102-LF-014-6603          UNCLASSIFIED

i

Analysis of the Effects of Ionospheric Sampling of Reflection Points Near-Path for High-Frequency Single-Site-Location Direction Finding Systems

by

Carlos Augusto Teixeira Filho
Lieutenant Colonel, Brazilian Army
B.S., Military Institute of Engineering - Brazil, 1977

Submitted in partial fulfillment
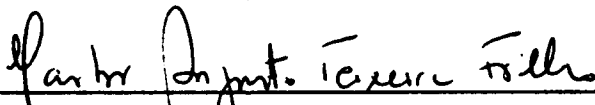of the requirements for the degree of

MASTER OF SCIENCE IN SYSTEMS ENGINEERING
(ELECTRONIC WARFARE)

from the
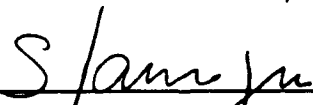
NAVAL POSTGRADUATE SCHOOL
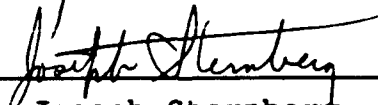December 1990

Author: _____
Carlos Augusto Teixeira Filho

Approved by: _____
Richard W. Adler, Thesis Advisor

_____
Stephen Jauregui, Jr, Second Reader

_____
Joseph Sternberg, Chairman
Electronic Warfare Academic Group

ii

# ABSTRACT

This thesis suggests a method to estimate the current value of an ionospheric parameter. The proposed method is based on the known variability of the observed current values near path and utilizes data derived from ionospheric sampling measurements. Analysis of errors is provided in Single-Site-Location High-Frequency Direction Finding (SSL-HFDF), arising from ionospheric irregularities such as Es (sporadic E), ionospheric tilts, and traveling ionospheric disturbances (TIDs). The characteristics of Es, tilts and TIDs for mid-latitudes are summarized in tables. The spatial and temporal coherence of ionospheric variabilities and irregularities is analyzed over the electron density. Practical results, measurements, and studies are presented on SSL-HFDF. A survey of characteristics of the ionosphere in the equatorial region is also provided. Finally, some recommendations are given to maximize the applicability of the proposed method.

iii

# TABLE OF CONTENTS

## ACKNOWLEDGMENT

I wish to thank Dr Richard W. Adler for his helpful suggestions, patience and support throughout my thesis research.

Special thanks must go to my wife, Maria Delfina, whose encouragement effort made my task much lighter.

# I. INTRODUCTION

## A. MULTIPLE SITE HIGH FREQUENCY DIRECTION FINDING

Interception of high frequency (HF) communications is one means of gaining additional intelligence in a military engagement. The interception of HF communications can also be used to locate the emitter, the knowledge of which may be of strategic or tactical value. Early radio direction finding employed geometrical triangulation. Geometrical triangulation involves the measurement of the bearing or azimuth angle of arrival (measured clockwise from the geographic north) of the target signal.

A network of at least two bearing measuring stations is often used to locate HF emitters. Position is usually derived from the intersection of two or more bearing estimates which are assumed to be straight line ray paths. Fixing accuracy is increased by using more than two direction finding (DF) stations and indicates how closely the intersections of the various rays coincide. The most likely source location is derived by a geometrical center-of-gravity (see Figure 1). In Figure 1, "FIX n/m" means fix using the DF stations DFn and DFm.
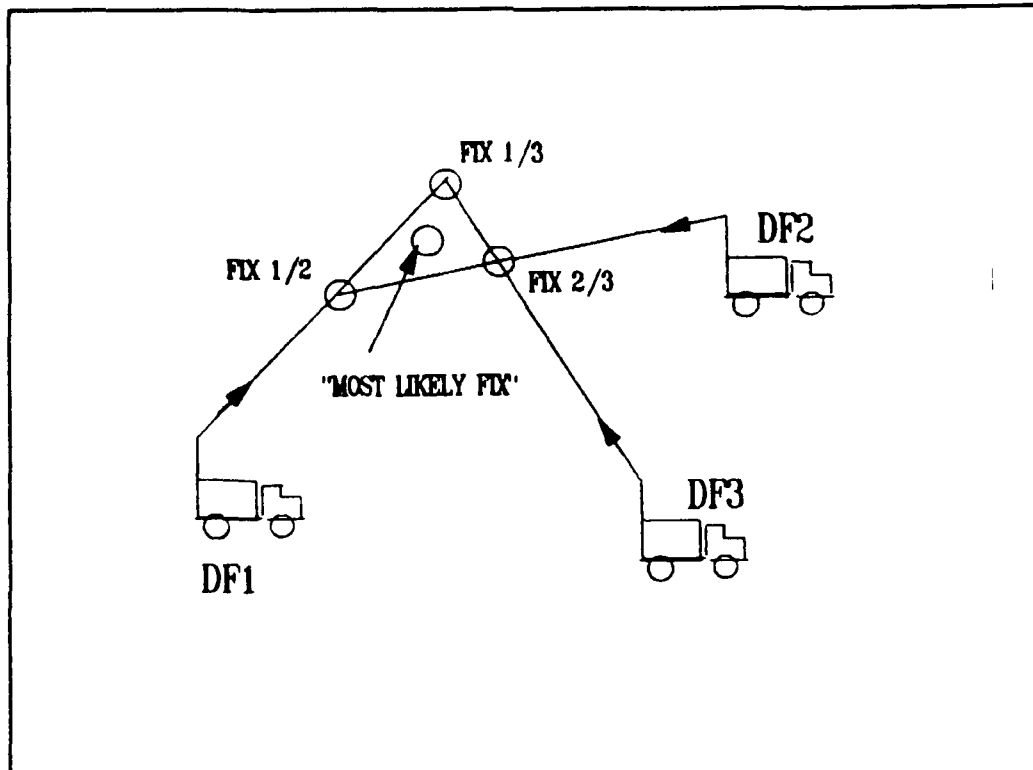
Figure 1   Multiple Site Location concept

The validity of the straight-line path assumption as well as the accuracy of the azimuthal angle-of-arrival (AOA) measurements regulate the degree of coincidence of various ray intersections and hence the fixing accuracy.

At frequencies between 3 and 30 MHz, over paths extending well beyond the optical horizon, the straight-line ray path assumption is not always valid. The most likely mode of propagation in this situation is typically the skywave or ionospherically propagated wave.

When assuming horizontal stratification of the refracting portion of the ionosphere, the ray will bend back toward the

2

earth along a path within the plane of incidence and the straight-line ray path remains valid. Unfortunately horizontal stratification is only a first-order approximation of the ionosphere. Large ionization gradients are present because of the direct effect of solar radiation on the ionosphere, and/or ionospheric disturbances of various scales and magnitudes. Lateral deviations in the ray path occur because of ionization gradients which have components transverse to the ray path, invalidating the straight-line ray path assumption. It seems evident that substantial fixing errors remaining in the HF geometrical triangulation procedure are due largely to lateral deviations in the ionospherically propagated ray path.

## B. SINGLE SITE HIGH FREQUENCY DIRECTION FINDING

The predominant method for radio wave propagation at HF is ionospheric reflection. The use of SSL-HFDF techniques requires compensation for the lateral deviation error inherent in the triangulation of skywave signals and to avoid the tactical problem of installing and coordinating angle-of-arrival measurements at two or more widely separated DF stations.

SSL-HFDF is one technique employed to solve the problem of determinating the location (fixing) of HF emitters. As the SSL-HFDF station makes angle measurements in the vertical and horizontal plane (see Figure 2), the location of the emitter is evaluated by the combination of: (1) The measured bearing

3

(azimuthal angle measurement that was previously required in the triangulation techniques); (2) The observed angle-of-elevation (the angle made by the arriving ray with the ground at the SSL-HFDF station); (3) Ionospheric models available; and (4) Raytracing techniques.
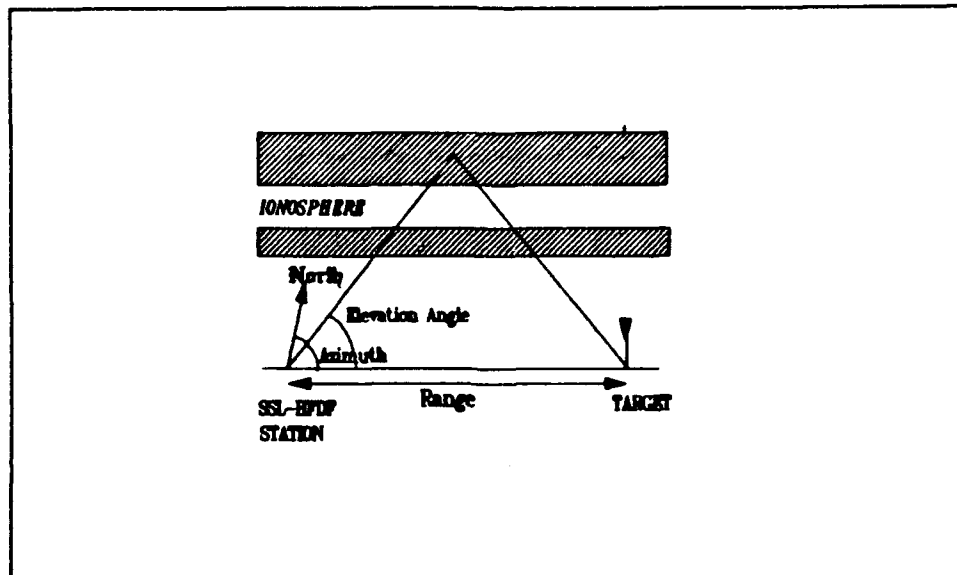


Figure 2  Single Site Location concept

The emitter's location is obtained by measuring the azimuth bearing and the range is calculated by tracing a ray at the observed angle of elevation back towards the emitter, using appropriate ionospheric models and raytracing techniques [Ref. 1].

Any emitting HF source yields two types of waves: one which propagates along the earth-air interface (the surface wave or groundwave) and the other which propagates through the

4

atmosphere (the direct wave), eventually to be reflected off the ionosphere (the skywave). The proportion of the one wave to the other for any given emitter depends on antenna design, orientation, distance and ground conditions. The groundwave is the strongest signal received, when the distance is 20 km to 100 km, depending on the topography, soil type, and soil conductivity. In this region the reflected skywave is of near-vertical incidence and yields little useful range or direction information. For short-distance HFDF, a system utilizing the groundwave would be the most applicable. At ranges greater than 100 km, and most optimally at ranges of a few hundred kilometers, the ground-based HFDF system using skywave should be employed. Skywave propagation is fundamental to understanding the SSL-HFDF process [Ref. 2].

## C. THE ROLE OF THE IONOSPHERE

The ability to trace the ray through the ionosphere depends on the accuracy of the model of the refracting portion of the ionosphere. In particular, knowledge of the vertical electron density profile in the proximity of the refracting ray is imperative.

Distribution of electron density in the ionosphere is strongly affected by the presence of horizontal gradients that cause more problems than in the case of the triangulation. Accuracy of a resulting fix by the SSL-HFDF system is directly affected by the longitudinal as well as the transverse

components of horizontal ionization gradients. Transverse components affect the estimate of the bearing of the target from the SSL-HFDF site, while the longitudinal components affect the estimate of the range of the target from the site. The backward ray-tracing procedure must rely upon incomplete information regarding the current status of the ionosphere as a consequence of spatial and temporal ionospheric variations.

## II. REFRACTION POINT ESTIMATION ANALYSIS

### A. GENERAL

For ideal performance of the SSL-HFDF station, near-real-time information is required on the state of the ionosphere. Ionospheric sounding is most frequently used to accomplish this in the region near the path. Quantifying the spatial and temporal irregularities of the ionosphere becomes very important. Equally important is the estimation of spatial and temporal ranges, which allow ionospheric sounding information gathered at one point to be extrapolated to another point with minimal loss of position location accuracy.

The fundamental question is, "If the state of the ionosphere can be determined at one particular point, over what spatial ranges can that information be transferred, and for what time period is it valid ?" [Ref. 6].

The principal aim of this chapter is to present, in theory, one process for the estimation of the current value of an ionospheric parameter. The applicability of this process should be investigated by using real ionospheric data measurements, which were not available for this research.

The limitations concerning spatial ranges and time period will be discussed in the final chapter.

## B. THE ESTIMATION PROCESS

### 1. Introduction

The problem considered here is that of estimating the current value of an ionospheric parameter on the basis of observed current values of the parameter at other locations.

In this study the following notations and assumptions will be made:

- The location for which the estimation is to be performed is given the label 0;

- The locations for which current observed values are available are designated 1,2,3,...n;

- The expected value (mean) and the variance of the parameter at each location 0,1,2,3,...,n are assumed to be known;

- The covariance of the parameter between each pair of locations is assumed to be known.

The way to estimate the previous parameters can be summarized as follows:

- The mean value at location 0 may be estimated in term of the median using the available ionospheric predictions published by specialized organizations around the world;

- The variance at location 0 is estimated from the geographical dependence observed in the variance at the other locations;

- The covariances involving 0 are estimated from the distance dependencies [Ref. 3].

## 2. Expected Values and Variances

Estimation of the deviation of a particular parameter from its mean value at location 0 is as described in the following analysis [Ref. 3].

It is necessary to calculate the predicted current deviation $x_p$ at 0, which is assumed to be a linear function of the observed current deviations at the n other locations, i.e.,

$$x_p = n^{-1}( k_1x_1+k_2x_2+\ldots+k_nx_n ) = n^{-1} \sum_{i=1}^{n} k_ix_i \quad , \qquad (1)$$

where

$x_i$ are the observed deviations,

$k_i$ are the prediction coefficients, and

n is the number of the location.

The goal is to minimize D, the expected mean square prediction error at 0, which is given by

$$D = (x_p-x_0)^2 \quad , \qquad (2)$$

where $x_0$ represents the true deviation at 0.

Then

$$D = \overline{[( n^{-1} \sum_{i=1}^{n} k_i x_i ) - x_0 ]^2} \quad , \tag{3}$$

Where the bar over the expression represents the mean or expected value.

To minimize D, the partial derivatives with respect to the n $k_i$'s must be zero. Thus, the solution of the following system of n equations yields the ideal values for the $k_i$

$$\frac{\partial D}{\partial k_1} = 2 \overline{[( n^{-1} \sum_{i=1}^{n} k_i x_i ) - x_0 ] ( n^{-1} x_1 )} = 0 \quad , \tag{4}$$

$$\frac{\partial D}{\partial k_2} = 2 \overline{[( n^{-1} \sum_{i=1}^{n} k_i x_i ) - x_0 ] ( n^{-1} x_2 )} = 0 \quad , \tag{5}$$

$$\cdot$$

$$\cdot$$

and

$$\frac{\partial D}{\partial k_n} = 2 \overline{[( n^{-1} \sum_{i=1}^{n} k_i x_i ) - x_0 ] ( n^{-1} x_n )} = 0 \quad . \tag{6}$$

**a.  Case 1 (One location)**

When estimating a parameter at location   0 with only one location (n=1):

$$k_1 \overline{x_1^2} - \overline{x_0 x_1} = 0 \qquad\qquad (7)$$

or

$$k_1 = \frac{\overline{x_0 x_1}}{\overline{x_1^2}} = \frac{\overline{x_0 x_1}}{\overline{x_1 x_1}} \qquad . \qquad\qquad (8)$$

If

$$s_{ij} = \overline{x_i x_j} \qquad , \qquad\qquad (9)$$

then

$$k_1 = \frac{s_{01}}{s_{11}} \qquad , \qquad\qquad (10)$$

where

$s_{01}$ is the covariance between locations 0 and 1, and

$s_{11}$ is the variance at location 1.

The constant $k_1$ can also be described as a function of the correlation coefficient $r_{01}$.

So from

$$r_{01} = \frac{Cov(0,1)}{\sqrt{S_{00}}\sqrt{S_{11}}} \quad , \tag{11}$$

$$Cov(0,1) = S_{01} = r_{01}\sqrt{S_{00}}\sqrt{S_{01}} = r_{01}\sigma_0\sigma_1 \quad , \tag{12}$$

and hence

$$S_{11} = \sigma_1^2 \quad . \tag{13}$$

The coefficient $k_1$ can be defined as

$$k_1 = r_{01}\left(\frac{\sigma_0}{\sigma_1}\right) \quad , \tag{14}$$

where the correlation coefficient $r_{01}$ between locations 0 and 1 [Ref. 4], is given by

$$r_{01} = \frac{COV(0,1)}{\sqrt{S_{00}}\sqrt{S_{11}}} = \frac{S_{01}}{\sqrt{S_{00}}\sqrt{S_{11}}} \quad . \tag{15}$$

If $s_{00}$, the variance at 0, is equal to $s_{11}$, then

$$r_{01} = \frac{s_{01}}{\sqrt{s_{11}^2}} = \frac{s_{01}}{s_{11}} \quad , \tag{16}$$

$$k_1 = r_{01} \quad . \tag{17}$$

Hence the mean square error D can be calculated as

$$D = [\ k_1 x_1 - x_0\ ]^2 = [\ r_{01} x_1 - x_0\ ]^2 = r_{01}^2 x_1^2 - 2 r_{01} x_1 x_0 + x_0^2 \tag{18}$$

$$= x_0^2 \left[\ r_{01}^2 \frac{x_1^2}{x_0^2} - 2 r_{01} \frac{x_1 x_0}{x_0^2} + 1\ \right] \quad , \tag{19}$$

where:

$$\frac{x_1^2}{x_0^2} = \frac{x_1 x_1}{x_0 x_0} = \frac{s_{11}}{s_{00}} = 1 \tag{20}$$

and

$$\frac{x_1 x_0}{x_0 x_0} = \frac{s_{10}}{s_{00}} = \frac{s_{01}}{s_{11}} = r_{01} \quad , \tag{21}$$

so that

$$D = x_0^2\ [\ r_{01}^2 - 2 r_{01}^2 + 1\ ] = x_0^2\ [\ 1 - r_{01}^2] \tag{22}$$

$$= s_{00}\ (1 - r_{01}^2) \quad . \tag{23}$$

13

Finally,

$$D = \sigma_0^2 (1 - r_{01}^2) \quad , \tag{24}$$

where

$\sigma_1^2$ is the variance at location 1.

### b. Case 2 (Two locations)

When estimating 0 with two locations (n=2):

$$\frac{\partial D}{\partial k_1} = \frac{2 \left[ \frac{1}{2} (k_1 x_1 + k_2 x_2) - x_0 \right] x_1}{2} = \frac{1}{2} (k_1 \overline{x_1^2} + k_2 \overline{x_1 x_2}) - \overline{x_0 x_1} \tag{25}$$

and

$$\frac{\partial D}{\partial k_2} = \frac{2 \left[ \frac{1}{2} (k_1 x_1 + k_2 x_2) - x_0 \right] x_2}{2} = \frac{1}{2} (k_1 \overline{x_1 x_2} + k_2 \overline{x_2^2}) - \overline{x_0 x_2} \quad . \tag{26}$$

We have

$$\frac{\partial D}{\partial k_1} = 1/2 (k_1 s_{11} + k_2 s_{12}) - s_{01} = 0 \tag{27}$$

and

$$\frac{\partial D}{\partial k_2} = 1/2 (k_1 s_{12} + k_2 s_{22}) - s_{02} = 0 \quad , \tag{28}$$

14

so that

$$k_1 = \frac{2\left[\left(\dfrac{S_{01}}{S_{11}}\right) - \left(\dfrac{S_{02}}{S_{12}}\right) r_{12}^2\right]}{(1 - r_{12}^2)} \qquad (29)$$

$$k_2 = \frac{2\left[\left(\dfrac{S_{02}}{S_{22}}\right) - \left(\dfrac{S_{01}}{S_{12}}\right) r_{12}^2\right]}{(1 - r_{12}^2)} \quad , \qquad (30)$$

$$D = \overline{\left[\frac{1}{2}(k_1 x_1 + k_2 x_2) - x_0\right]^2} \qquad (31)$$

$$= \frac{1}{4}(k_1^2 \overline{x_1^2} + k_2^2 \overline{x_2^2}) + \frac{1}{2} k_1 k_2 \overline{x_1 x_2} + \overline{x_0^2} - k_1 \overline{x_0 x_1} - k_2 \overline{x_0 x_2} \quad , \qquad (32)$$

hence,

$$D = \frac{1}{4}(k_1^2 S_{11} + k_2^2 S_{22}) + \frac{1}{2} k_1 k_2 S_{12} + S_{00} - k_1 S_{01} - k_2 S_{02} \quad . \qquad (33)$$

Solution of this system when n=2 can be simplified by assuming equal variances,

$$S_{11} = S_{22} = S_{00} = S_{xx} \quad , \qquad (34)$$

and equal covariances with respect to 0,

$$S_{01} = S_{02} = S_{0x} \quad , \qquad (35)$$

15

so that

$$k_1 = k_2 = k_x = \frac{2S_{0x}}{(S_{xx}+S_{12})} \quad , \tag{36}$$

and

$$D = \frac{1}{2}k_x^2(S_{xx}+S_{12}) + S_{xx} - 2k_xS_{0x} \quad , \tag{37}$$

which, substituting for $k_x$, gives

$$D = 2\frac{S_{0x}^2}{(S_{xx}+S_{12})} + S_{xx} - 4\frac{S_{0x}^2}{(S_{xx}+S_{12})} = S_{xx} - 2\frac{S_{0x}^2}{(S_{xx}+S_{12})} \tag{38}$$

$$= S_{xx}\left[1-\left[\frac{S_{0x}^2}{S_{xx}^2}\right]\left[\frac{2}{(1+\frac{S_{12}}{S_{xx}})}\right]\right] = S_{xx}\left[1-r_{0x}^2\left[\frac{2}{1+r_{12})}\right]\right] \quad . \tag{39}$$

This formula reduces to the case n=1 when $r_{12}=1$.

### c. Case 3 (Multiple locations)

When the prediction is based upon observations at more than one location, the general approach to the expected mean square prediction error (See Appendix A) is:

16

$$D = \sigma_0{}^2 \, (1 - R_{0n}{}^2) \quad , \tag{40}$$

where $R^2{}_{0n}$ is the coefficient of multiple correlation of $x_0$ with relation to $\{ x_1, x_2, \ldots, x_3 \}$.

## C.  SUMMARY OF THE ESTIMATION PROCESS

**1st STEP**: Calculate the variance ($\sigma_i{}^2$) of the parameter at each location $i=1, 2, \ldots, n$ given by the formula

$$\sigma_i^2 = \frac{\sum_{i=1}^{n} (x_i - \mu_i)^2}{n-1} = \frac{\sum_{i=1}^{n} x_i^2 - \dfrac{\left(\sum_{i=1}^{n} x_i\right)^2}{n}}{n-1} \quad , \tag{41}$$

where   $n$ = number of measurements at location $i$,

$x_i$ = measurement at location $i$, and

$\mu_i$ = mean value of the observations at location $i$
[Ref. 4].

**2nd STEP**: Calculate the variance ($\sigma_i{}^2$) of the parameter at location 0 as in the first step or, when no measurements are available, estimate its value from the spatial (geographical) interpolation of the variances at locations $i=1, 2, \ldots, n$.

**3rd STEP**: Calculate the covariances and the correlation coefficients for each pair of locations including location 0.

The correlation coefficient $(r_{xy})$ is the simple linear correlation coefficient given by the formula [Ref. 5]

$$r_{xy} = \frac{n\left(\sum_{i=1}^{n} xy\right) - \left(\sum_{i=1}^{n} x\right)\left(\sum_{i=1}^{n} y\right)}{\sqrt{n\left(\sum_{i=1}^{n} x^2\right)-\left(\sum_{i=1}^{n} x\right)^2}\sqrt{n\left(\sum_{i=1}^{n} y^2\right)-\left(\sum_{i=1}^{n} y\right)^2}} \quad . \tag{42}$$

The covariance $(COV(X,Y))$ for each pair of locations is given by the formula [Ref. 4]

$$COV(X, Y) = r_{xy}\sqrt{\sigma_x^2\sigma_y^2} = s_{xy} \quad . \tag{43}$$

**4th STEP**: Solve the correlation matrix (see Appendix A) and calculate the prediction coefficients $(k_j)$ and the coefficient of multiple correlation $(R_{0n}^2)$

$$k_j = n\frac{C_{0j}}{C_{\upsilon 0}} \qquad (j = 1, 2, \ldots, n) \tag{44}$$

$$R_{0n}^2 = 1 - \frac{|S|}{s_{00}C_{00}} \quad . \tag{45}$$

18

**5th STEP**: Calculate the current deviation $(x_i)$ of the parameter for each location $i=1,2,\ldots,n$.

$$x_i = m_i - \mu_i \quad , \tag{46}$$

where   $x_i$ = deviation of the ith measurement from the mean (ith deviation);

   $m_i$ = measured or observed value at location i;

   $\mu_i$ = actual mean value at location i.

**6th STEP**: Calculate the estimated deviation $(x_p)$ of the parameter at location 0:

$$x_p = \frac{1}{n}\sum_{i=1}^{n} k_i x_i \quad . \tag{47}$$

**7th STEP**: Calculate the predicted value (P) of the parameter:

$$P = \frac{1}{n}\sum_{i=1}^{n} m_i + x_p \quad . \tag{48}$$

**8th STEP**: Calculate the expected mean square prediction error (D) for one station and for multiple stations.

For one location, the error is

$$D = \sigma_0^2 (1 - r_{01}^2) \quad , \tag{49}$$

and for multiple locations it is:

$$D = \sigma_0^2 (1 - R_{0n}^2) \quad , \tag{50}$$

where   $r_{01}$ = Correlation coefficient between locations 0 and 1, and

$R_{0n}$ = Multiple correlation coefficient among location 0 and locations $1, 2, \ldots, n$.

# III. ANALYSIS OF ERRORS IN SSL-HFDF

## A. OVERVIEW

Current SSL-HFDF systems occasionally produce errors of tens of kilometers or worse. These errors arise from three main areas: ionospheric variability and irregularity, locator system size limitations, and problems with data acquisition, processing and interpretation. Of these areas the ionosphere is the single largest source of error.

Measurement of the azimuthal and elevation angles of the incoming signal and determination of the height of the ionospheric reflecting layer are, in principle, the procedures used to locate the HF emitter.

In practice, there are several types of ionospheric irregularities which distort the otherwise straightforward picture of a uniform, concentric, smoothly-reflecting ionosphere. Three phenomena can be pointed out because of their significance among various causes of irregularities and their effects on SSL-HFDF: sporadic E (Es), ionospheric tilts, and traveling ionospheric disturbances (TIDs).

### 1. Sporadic E (Es)

Because of the thickness of the layers and the sharpness of the vertical gradients, Sporadic E is often an aid in communication and often provides a better reflection

surface than the F region. Unfortunately, the inconvenience of Es is that it introduces uncertainty as to which ionospheric layer, E or F, is reflecting the signal and provides additional opportunities for multimode reflections of signals. Signals from the source may suffer reflections from both E and F layers, thus causing additional problems with resolution or modes.

The properties of Es are summarized in Table I [Ref. 6] for the mid-latitudes.

TABLE I - PROPERTIES OF Es FOR THE MID-LATITUDES

| Structure | (1) Patches of enhanced electron and ion density often hundreds of km in horizontal extent.<br>(2) Vertical thickness generally 1-2 km at an altitude of 100-110 km.<br>(3) Patches of high density often embedded in larger, lower density patches. |
|---|---|
| Origin | Wind shears, probably from propagating acoustic-gravity waves. |
| Motion | Patches (not plasma) generally move 50-100 m/s, no preferred direction. |
| Duration | Several minutes to several hours. |
| Occurrence | (1) More frequent during day, with peak occurrence before noon, and in some locations a secondary peak near sunsets likely in summer.<br>(2) Frequency of occurrence (detection) more likely for lower radio frequencies. |

## 2. Ionospheric Tilts

Ionospheric tilts refer to any deviation from the horizontal plane of the contours of constant electron density,

22

whether caused by large-scale phenomena such as solar ionization, or due to more transient and localized TIDs.

Miscalculation of the virtual height of the reflection point, and error in estimating the angle of arrival, in particular the elevation angle, are the dominant effects of ionospheric tilts.
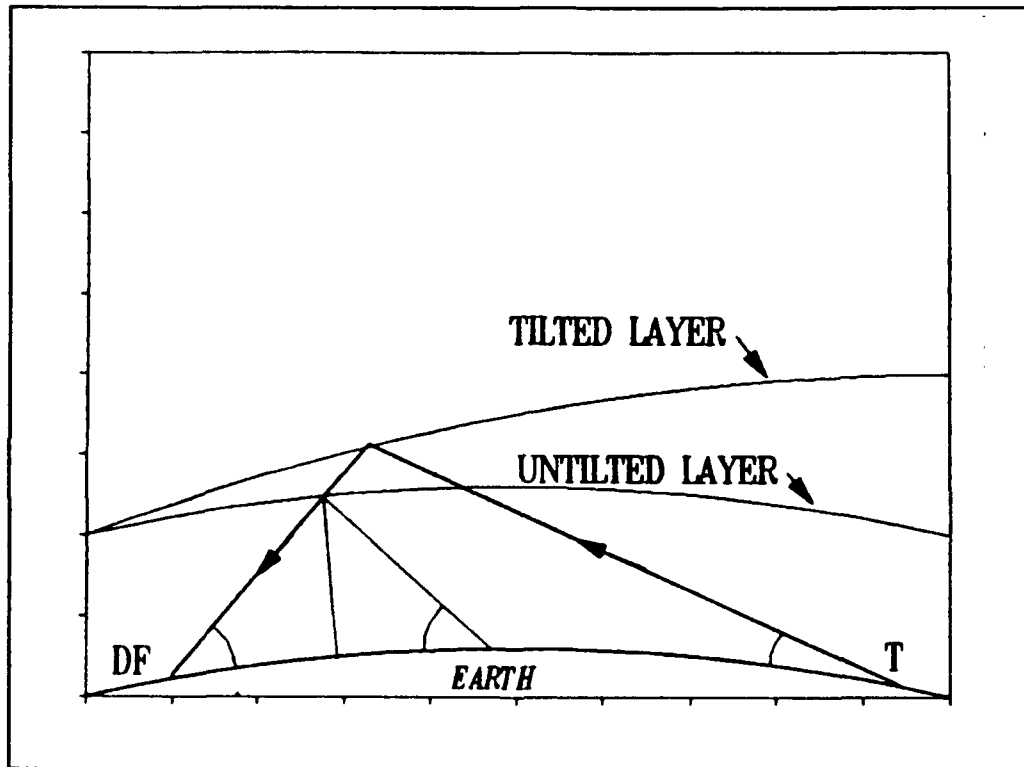


Figure 3  Effect of a Longitudinal Tilt component

The diurnally-varying solar ionization rate in the F region causes the most regular and predictable ionospheric tilt. This is most observable at sunrise and sunset, so it can be predicted and described [Ref. 6].

23

The properties of ionospheric tilts are summarized in Table II [Ref. 6] for the mid-latitudes.

TABLE II - PROPERTIES OF IONOSPHERIC TILTS FOR THE
MID-LATITUDES

| | |
|---|---|
| Structure | (1) Horizontal gradient in electron density over distances on the order of 1000 km.<br>(2) Found at F region altitudes (>140 km). |
| Origin | Daily variation of solar ionizing radiation. |
| Motion | Pattern shifts with sun's diurnal motion. |
| Duration | On the order of 1-2 hours. |
| Occurrence | Daily near sunrise and sunset. |

### 3. Traveling Ionospheric Disturbances (TIDs)

Errors in the measured azimuthal and elevation angles (angles of arrival), and in the virtual height of reflection are the main effects of TIDs.

The spectrum of TIDs can be placed in at least three distinct categories: large-scale, medium-scale and small-scale [Ref. 6].

- Large-scale TIDs, according to acoustic wave theory, are associated with a discrete spectrum of guided waves whose modes are excited only by upper atmospheric sources and whose horizontal speeds are substantially greater than the (lower atmospheric) speed of sound.

- Medium-scale TIDs are associated with a spectrum of freely-propagating internal waves which can be excited by sources at any altitude and whose horizontal speeds are less than the speed of the sound. Medium-scale TIDs are much more common.

24

- Small-scale TIDs are more likely the extension to higher frequencies and smaller size of the medium-scale TIDs. They are generally below the Fresnel-zone size of ionospheric sounders and thus have not been as well documented.
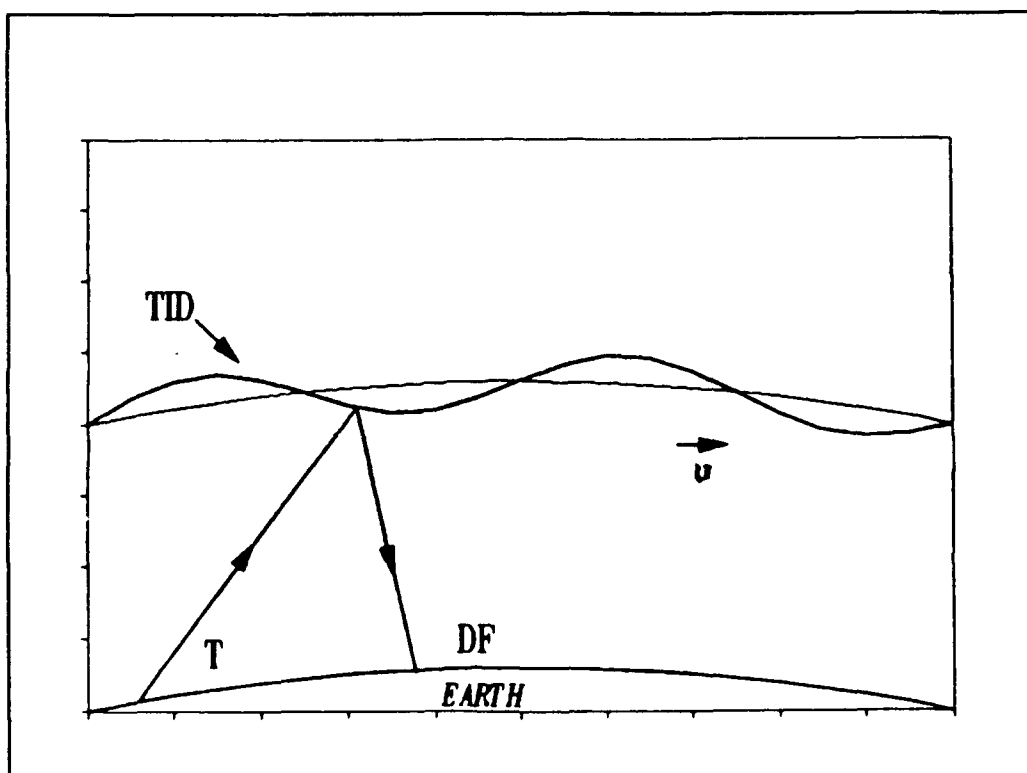


Figure 4   Traveling Ionospheric Disturbance (TID)

Table III [Ref. 6] summarizes the properties of these different categories, and Table IV [Ref. 6] gives the magnitude of the errors in position location which the ionosphere can cause for selected ranges. A quick "rule of thumb" seems to be 10 km or 10% of range, whichever is worse [Ref. 6].

## TABLE III - PROPERTIES OF TIDs

| TID | LARGE-SCALE | MEDIUM-SCALE | SMALL-SCALE |
|---|---|---|---|
| Wavelength and structure | (1) >1000km horizontal wavelength<br><br>(2) Wave-front width near 1000 km<br>(3) Phase fronts tilted nearly horizontal<br>(4) Retains shapes over 1000s km | (1) 10s to 100s km horizontal wavelength<br>(2) Wave-front width 100s to 1000 km<br>(3) Phase fronts tilted 30°-60° from vertical<br>(4) Do not retain shapes at d>100 km | (1) <10 km horizontal wavelength<br><br>(2)Structure not well resolved |
| Motion | > 300 m/s North to South | 100-250 m/s variable directions with seasonal trends | 100-250 m/s (estimated) variable directions |
| Period | 30 min.-3 hr. usually 1-3 cycles | 10-100 min., several cycles to trains | <10 min. long, trains to families as wavelength decreases |
| Frequency of Occurrence | Infrequent, less than daily | Daily, more common daytime | Daily |
| Source | (1) Events in the auroral zone<br>(2) Strong correlation with magnetic activity | (1) Tropos-pheric phenomena<br><br>(2) Upper atmospheric & polar winter sources | (1) Probably tropospheric (not well established) |

27

TABLE IV - MAGNITUDE OF ERRORS IN HFDF DUE TO ERRORS IN AOA
FOR E AND F LAYERS

| ACTUAL RANGE (km) | 200 | | 300 | |
|---|---|---|---|---|
| HEIGHT OF REFLECTING LAYER (km) | 105 | 250 | 105 | 250 |
| Range Error (km) for: | | | | |
| 1° elevation angle uncertainty | 6.9 | 9.8 | 10.9 | 11.5 |
| 3° elevation angle uncertainty | 20.6 | 29.3 | 32.7 | 34.4 |
| Cross-Range (Azimuthal) Error (km) for: | | | | |
| 1° azimuthal angle uncertainty | 3.5 | 3.5 | 5.2 | 5.2 |
| 3° azimuthal angle uncertainty | 10.5 | 10.5 | 15.6 | 15.6 |
| Range Error (km) for: | | | | |
| 10 km height uncertainty | 19.4 | 7.7 | 27.6 | 11.5 |

## B. SPATIAL AND TEMPORAL COHERENCE OF IONOSPHERIC VARIABILITIES AND IRREGULARITIES

### 1. Electron Density: Temporal and Spatial Variabilities

The ionosphere displays variation in electron density on many temporal scales. The 11-year solar cycle dependency in addition with the seasonal and monthly changes in electron density are the most useful scale references.

The day-by-day variability is the most difficult to model. As an example, some studies show that the variability of daily hourly values of foE and foF1 (see Glossary) about the monthly hourly values expressed in terms of the standard deviation is on the order of 5 to 10 percent. The same study

provides evidence that the daily variability of foF2 (see Glossary) is between 10 and 20 percent [Ref. 7].

The equatorial and polar regions of the globe show a daily variability stronger than that in mid-latitude locations. This phenomena is attributed to the daily variability observed in processes such as electrodynamic drift, diffusion, neutral-air winds, and particle precipitation that compete for control of the ionization distribution in the low- and high-latitude F region.

It is very important to emphasize that the height of the maximum electron density (hm) in the different ionospheric regions also varies with time and location, and the hmF2 tends to show the most significant changes of all the ionospheric maximum heights. At mid-latitudes, hmF2 is usually on the order of 300 to 400 km during nighttime hours and between 250 and 350 km during daytime hours, whereas at equatorial latitudes, the daytime values are 100 to 150 km higher than the nighttime values.

Regardly spatial variability, the electron density is dependent on the solar zenith angle, as a general rule, and its maximum latitudinal distribution is a maximum near the sub-polar point. The F region and E region (Es) have a significant latitudinal dependence, and in the F2 region, the electron density displays complicated latitudinal behavior [Ref. 8].

## 2. Electron Density Irregularities

The analysis of the irregular electron density structures in the ionosphere in the F and E regions are summarized in Table V [Ref. 8].

TABLE V - IONOSPHERIC ELECTRON DENSITY IRREGULARITIES

| REGION | LATITUDE | IRREGULARITIES IN THE ELECTRON DENSITY |
|--------|----------|----------------------------------------|
| F | LOW | . In evening hours, continuing throughout night hours<br>. Tends to decrease during times of geomagnetic disturbances<br>. Significant longitudinal variability as well latitudinal and temporal dependencies<br>. Causes fading on HF circuits |
| | MIDDLE | . Associated with Spread F phenomenon<br>. Low magnitude, duration, and effect on communications system performance |
| | HIGH | . It appears more or less routinely<br>. More intense during hours of darkness<br>. Greater than at low latitudes<br>. It causes fading on HF circuits |
| E | LOW | . Generally are characterized as Es<br>. Present during high % of daytime<br>. Latitude of maximum occurrence varies with longitude |
| | MIDDLE | . Are generally characterized as Es, most frequently in summer daytime<br>. The diurnal variation has maxima in the mid-morning hours and near sunset |
| | HIGH | . Irregularities are quite common<br>. Associated with auroral activity are mainly a nighttime phenomenon, and when occurring in thick layers they produces radio wave retardation |

## 3. Practical Results on SSL-HFDF

The reflection point of the intercepted HF signal is far from the SSL-HFDF station. For a spatially and temporally uniform, or at least slowly varying ionosphere, this would introduce no problem. In reality, however, ionospheric irregularities reduce the usefulness of information gathered at one point when transferred to another point.

By cross-correlating the angle-of-arrival deviations of the signals received from pairs of geographically distinct emitters, and assuming a one-hop propagation path, some practical results can be obtained. When the variations in the angle of arrival at one location are reproduced at the second location "t" seconds later, the cross-correlation function is maximized. Interference between signals from different sources, or from the same source travelling different paths, or due to a single frequency component of the composite disturbance can result in the observed decorrelation.

Good spatial and temporal coherence are observed from ionospheric tilts due to solar influence or from large-scale TIDs, maintaining their shapes over long distances and for times on the order of one hour or more. The spectrum of medium-scale TIDs is superimposed on these migrating regular waves. The most frequently occurring ionospheric irregularities and the ones showing the least spatial and temporal coherence are the medium-scale TIDs, and these seem

31

to place the most rigorous limitations on accuracy when extrapolating the state of the ionosphere.

Sporadic E can be analyzed under the concepts of spatial and temporal coherence, or decorrelation, only when the patch length and the flux of the Sporadic E layer will give some estimate of how long the phenomenon is expected to remain at any one given point.

Table VI [Ref. 6] provides a summary of this group of properties for ionospheric irregularities.

TABLE VI - SUMMARY OF IONOSPHERIC IRREGULARITIES

| TYPE | SPATIAL DECORRELATION | TEMPORAL DECORRELATION | MAJOR EFFECTS |
|---|---|---|---|
| Es | ~100s km, depending on the size of the patch | Minutes to hours, depend. on relative location of patch & its drift veloc. | - Uncertainty in height of reflecting layer<br>- Multimode propagation |
| Ionospheric Tilt | 100s to 1000s km | Hour or longer | - Uncertainty in AOA and height of reflecting layer |
| Large-scale TID | 1000s km | 30 min to several hours | - Uncertainty in AOA and height of reflecting layer |
| Medium-scale TID | 50-100 km | ~5 minutes | - Uncertainty in AOA and height of reflecting layer<br>- Multimode propagation |

## C. EQUATORIAL REGION CONSIDERATIONS

The considerations discussed here do not give a thorough study of all problems of the equatorial ionospheric environment, a very intricate region, but they do reflect the current knowledgement of this medium and point out some of its characteristics:

(1) Large ionospheric F-region tilts occur along great circle paths leaving temperate regions and passing through equatorial regions in early evening hours. These tilts, both

positive and negative, range in angle from about 1° to 6° [Ref. 9];

(2) Very pronounced modifications of the modes of propagation of HF signals along paths traversing the equatorial regions in evening hours are produced by quite small tilts in the ionospheric F2 region [Ref. 9];

(3) The more important of the transequatorial tilt-mode propagation paths occur at low elevation angles. A high degree of ray-focusing commonly occurs for elevation angles below 8°. These focused modes lead to very stable backscatter echo configurations, such as are commonly observed for anomalous transequatorial echoes [Ref. 9];

(4) There is a permanent daytime belt of sporadic E of high critical frequency, which breaks up and disappears near sunset [Ref. 10];

(5) As the distance between two points increases, there is generally a decreased correlation between the parameters at the two points, tending to become negative at the distance of the stations near the magnetic equator [Ref. 11];

(6) The spread F is more likely occurs between about 2100 and 0100 local time, earlier when sunspots are at maximum. Its occurrence is greater during local summer than local winter. Its occurrence probability decreases with sunspot number [Ref. 16].

## IV. CONCLUSIONS AND RECOMMENDATIONS

### A. CONCLUSIONS

The applicability of the proposed method for estimating ionospheric parameters must be investigated using data measurements. The predicted values calculated should be compared to real measurements. For each particular environment (low, middle and high latitudes) the periodic_ty of the measurements and some adjustments in the model will certainly be necessary to find the optimum predicted parameter. (For example, in the equatorial region the predicted values should be calculated at sunrise, noon, sunset and nighttime).

### B. RECOMMENDATIONS

The following recommendations were found in technical reports and stem from several years of exhaustive research by specialized organizations. They relate to maximizing the applicability and making the proposed procedure operative for the estimation of ionospheric parameters.

(1) The validity of the ionospheric data taken at one point is lost when extrapolated over distances of 50-100 km or at periodicity greater than five minutes [Ref. 6].

(2) Data from a single ionosonde should never be used to model a large area of the ionosphere. The utilization of an integrated network of ionosondes is recommended using both vertical and oblique sounding [Ref. 6].

(3) Analysis of the relationship between $R_n^2$ ($R_n$ = coefficient of multiple correlation) and n (number of measurements or observations) for particular configurations indicates that the maximum value of $R_n$ (minimum value of the expected mean square prediction error D) tends to be reached at low values of n [Ref. 11]. This recommendation suggests the investigation of different ionosonde configurations to fit diverse tactical environments.

(4) Installation of the ionosonde at the anticipated mid-point of the propagation path is suggested to optimize the measurements. To find the best location for the SSL-HFDF system and ionosonde station, a preselection of range and detection is recommended over which the fixing will occur [Ref. 6];

(5) Measurement at different observation times is recommended to provide data for parameter estimation as a function of time in addition to simultaneous time geographical interpolation [Ref. 11];

(6) Implementation of an ionosonde network sometimes becomes impractical, as for example, in an ocean region or when the utilization of the output data may be not possible at near-real-time due to large networks. The suggested solution in these cases is to use techniques to obtain data from oblique ionograms by using oblique bistatic sounding or oblique backscatter sounding techniques [Ref. 12].

# APPENDIX A – GENERAL SOLUTION OF THE CORRELATION MATRIX

Let S represent the correlation matrix [Ref. 3];

$$
S \;=\; \begin{vmatrix} S_{00} & S_{01} & \cdots & S_{0n} \\ S_{10} & S_{11} & \cdots & S_{1n} \\ \cdots & \cdots & \cdots & \cdots \\ S_{n0} & S_{n1} & \cdots & S_{nn} \end{vmatrix} \;, \tag{51}
$$

where

$$
S_{ij} \;=\; \overline{X_i X_j} \;, \tag{52}
$$

$$
\frac{k_j}{n} \;=\; \frac{S_{0j}}{S_{00}} \;, \tag{53}
$$

$$
D \;=\; \frac{|S|}{C_{00}} \;, \tag{54}
$$

$$
C_{ij} \;=\; (-1)^{i+j} \, |M_{ij}| \;, \tag{55}
$$

and

$$
R_{0(1,2,\ldots,n)}{}^2 \;=\; R_{0n}{}^2 \;=\; 1 - \frac{D}{S_{00}} \;=\; 1 - \frac{|S|}{S_{00} C_{00}} \;; \tag{56}
$$

38

or

$$D = s_{00}[\ 1-R_{0n}{}^2\ ] = \sigma_0^2[\ 1-R_{0n}{}^2\ ]\quad , \qquad\qquad \textbf{(57)}$$

where

$S$ is the correlation matrix with rows (i) and columns (j) varying from 0 to n;

$C_{ij}$ is the cofactor of $s_{ij}$ in $|S|$; that is, the ijth cofactor of S is obtained by taking the determinant of the ijth minor $M_{ij}$ and multiplying it by $(-1)^{i+j}$ [Ref. 13];

$M_{ij}$ is the ijth minor of the n x n matrix S, and is defined as the (n-1) x (n-1) matrix obtained from S by deleting the ith row and jth column of S [Ref. 13];

$|S|$ is the determinant of S;

$s_{ij}$ is either the covariance between locations i and j (when i does not equal j), or the variance at location i, $\sigma^2_i$, (when i=j);

$R_{0(1,2,\ldots,n)}$, or $R_{0n}$, is the coefficient of multiple correlation of $x_0$ with $\{x_1,\ x_2,\ldots,\ x_n\}$; and

$D$ is the expected mean square prediction error.

## APPENDIX B - SKYWAVE PROPAGATION CONCEPTS

A complex reflection mechanism of ionospheric layers controls the propagation of skywaves. As shown in Figure 5, the propagating wave can be thought of as a ray reflecting alternately from the ionosphere and the ground. The wave generally follows several different paths at the same time, and this combination of paths is of major importance in the transmission of the signal's energy between two points. At any given time, the nature of this multipath propagation is also highly dependent on ionospheric conditions. Although it is called "reflection", the phenomenon which causes radio waves to change direction is not true reflection, but a case of strong refraction in a downward direction. As the magnitude of refraction depends upon the frequency, the effect of the refraction decreases with increasing frequency. Hence, there is critical frequency for a given ionospheric profile and angle of incidence, beyond which reflection back to earth cannot occur. According to observed radio properties, the ionosphere has been subdivided into three regions or layers, D, E, and F, increasing in altitude and in electron density.

The D region spans the altitude range 50 to 90 km, with electron density varying according to the solar zenith angle.
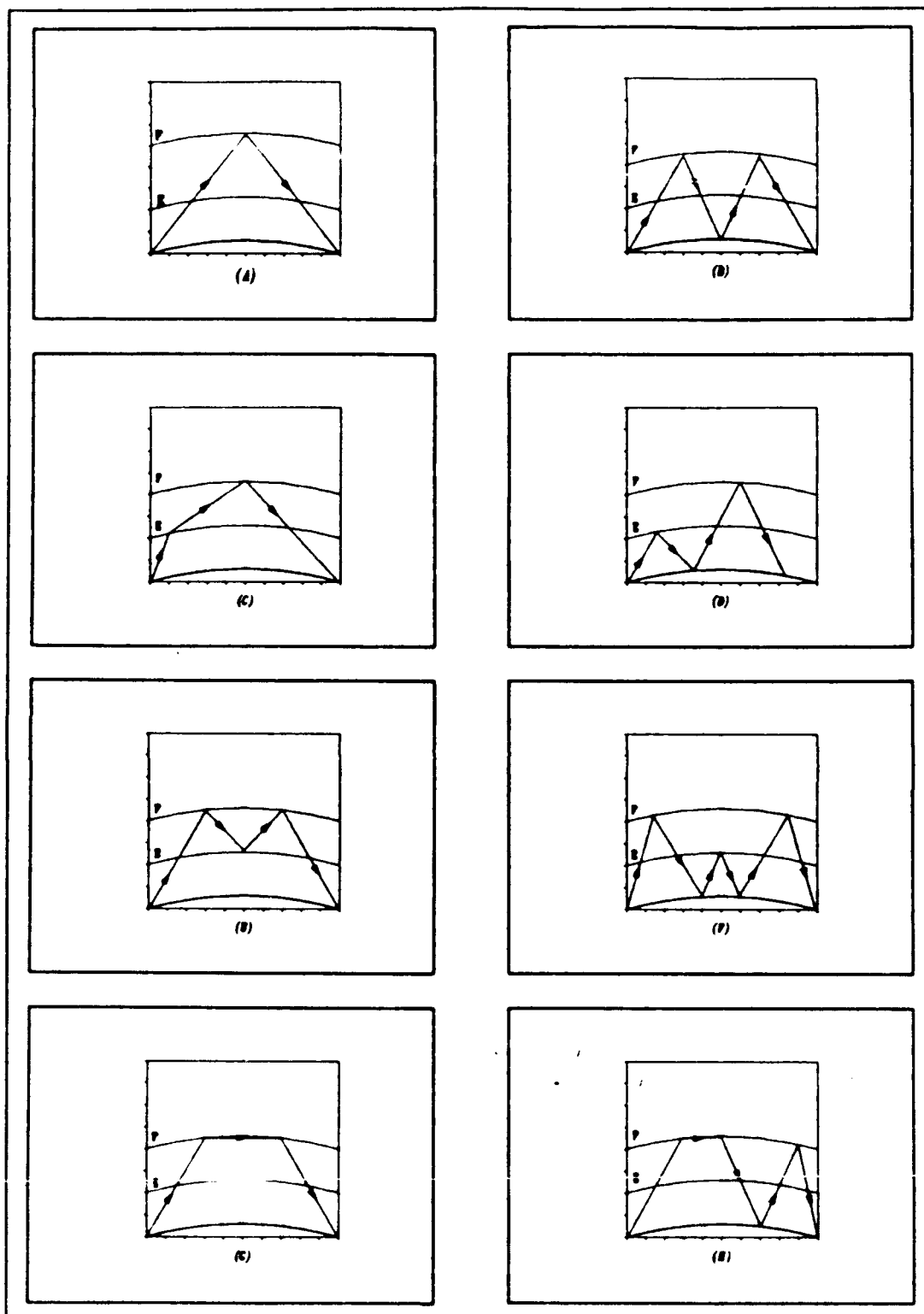
Figure 5   Types of Oblique Ray Paths

41

In the case of the HF spectrum, the D region acts principally as an attenuator of radio waves.

The E region ranges from 90 to 130 km in height, and the electron density encompasses the so-called "normal" and "sporadic E" ($E_s$) layers. The normal E layer has a strong solar zenith angle dependence, and the $E_s$ has a diurnal variation with location on the globe. The normal E acts as a reflector of HF waves, particularly during the daylight hours, and the electron density associated with $E_s$ acts by reflecting and/or scattering HF waves.

The F region is a thick region that extends upward from 130 km. It is subdivided into F1 and F2 layers because its lower part displays a different variation than the upper part. The F1 layer electron density reaches its maximum near local noon and during the summer. At night and during winter there is no distinction between F1 and F2 layers. The F2 layer displays the greatest electron density, and its electron density departs significantly from a simple solar zenith angle dependence, since it is strongly influenced by neutral-air winds, electrodynamic drifts, and diffusion processes. the maximum electron density tends to occur after local noon and its structure depends upon geomagnetic latitude. Long-distance HF circuits rely primarily upon reflection of radio waves from the F region during both day and night hours.

The altitude and density of the F-region peak determines the critical frequency for propagation. Especially where sharp gradients occur in the electron density profile, reflections at some frequencies can occur at altitudes well below this region peak.

The interaction of the radio waves with the ionization below the reflection region causes the energy which is given to the electrons to be lost in collisions with the neutral atmosphere. The effect of this loss of energy is the absorption of radio waves, and this absorption coefficient, which decreases with increasing frequency, achieves such a magnitude that propagation will obstruct signal reception.

In the presence of the earth's magnetic field and with its dispersive properties, the ionosphere becomes both anisotropic and doubly refracting. So, in this environment, the ionospheric index of refraction, which determines the radio wave properties at any point in the ionosphere, is a parameter which is a complex function of four independent variables that can be described as functions of five parameters: (1) the electron density of the ionosphere; (2) the atmospheric collision frequency; (3) the radio wave angular frequency; (4) the ionospheric angular gyrofrequency, and (5) the angle between the earth's magnetic field and the direction of the radio propagation.

By using Snell's Law, and given the index of refraction as a function of the radio wave position in the ionosphere, the

propagation of the radio wave can be traced by a form of the optical equation. By applying this law to ionospheric propagation, it can be stated that when the radio wave transverses an imaginary surface between two regions of the ionosphere having different refractive indices, $n_1$ and $n_2$, the refracted wave leaves the surface at an angle $\phi_2$, which is related to the radio wave angle of incidence with the surface, $\phi_1$, and the indices of refraction as follows:

$$\frac{\sin(\phi_1)}{\sin(\phi_2)} = \frac{n2}{n1} \quad . \tag{58}$$

The properties of the ionosphere are complex and quite unstable. These properties affect the ray path of the HF radio wave in the ionosphere, so a complete description of the ionosphere must take into account this variability, part of which is cyclic and follows predictable trends, and part of which is transient. These cyclic variations are due to the earth's rotation (day), to the rotation of solar active regions (30 days), to seasons (12 months), and cyclic variations in solar activity (11 years). The noncyclic variations are due to random changes in atmospheric properties, ionization transport by electrical current systems in the ionosphere, by large scale winds, and transient radiations from the sun. The noncyclic variations are

unpredictable. The only exceptions are some ionospheric effects produced by transient solar radiations.

Among the various anomalous conditions of the ionosphere that have been noted, one of the more important is the equatorial anomaly [Ref. 14].

## APPENDIX C - IONOSPHERIC SOUNDING

Ionospheric sounding is a technique used for sounding the ionospheric propagation medium characteristics. The following techniques have been developed for ionospheric sounding [Ref. 15]:

**Ionospheric Pulse Sounding**: This concerns the measurement of the linear unit impulse response function for each communications channel. The output of the sounder is usually displayed in the form of an ionogram. Three basic schemes are used:

1. Vertical Incidence Pulse Sounding: The sounding pulse is emitte' vertically and the reflected returns from the ionosph re are analyzed at a co-located or nearby receiver (Fig. 6).

2. Oblique Incidence Bistatic Pulse Sounding: The sounding pulse is emitted either over the actual communications path, or over an adjacent path. This method requires the transmitter and receiver to be remotely synchronized (Figure 7).

3. Oblique Incidence Backscatter Pulse Sounding: As with vertical sounding, the transmitter and the receiver are co-located or relatively close, but the received signals are reflected obliquely from the ionosphere and are scattered by ground irregularities (Figure 8).

**Linear Sweep Sounding or 'Chirpsounding'**: This consists of sending a low power, 2-30 MHz, linear FM/CW test signal over the communications path. The sounding signal is tracked by the time-synchronized receiver. It sounds the communications path obliquely and vertically (Figure 9).

**Channel Sounding**: This method uses probing transmissions on only a limited number of allocated frequencies over the radio link of interest. It is more correctly described as channel evaluation.
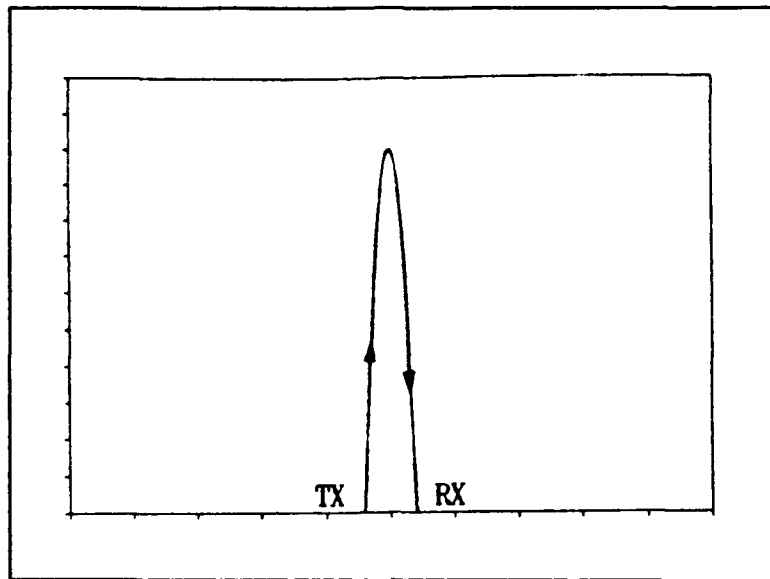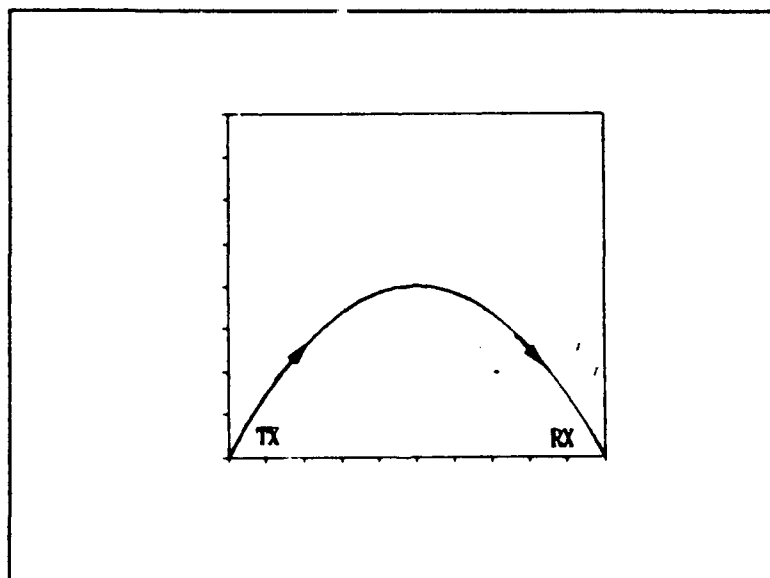
Figure 6 - Vertical Pulse Sounding
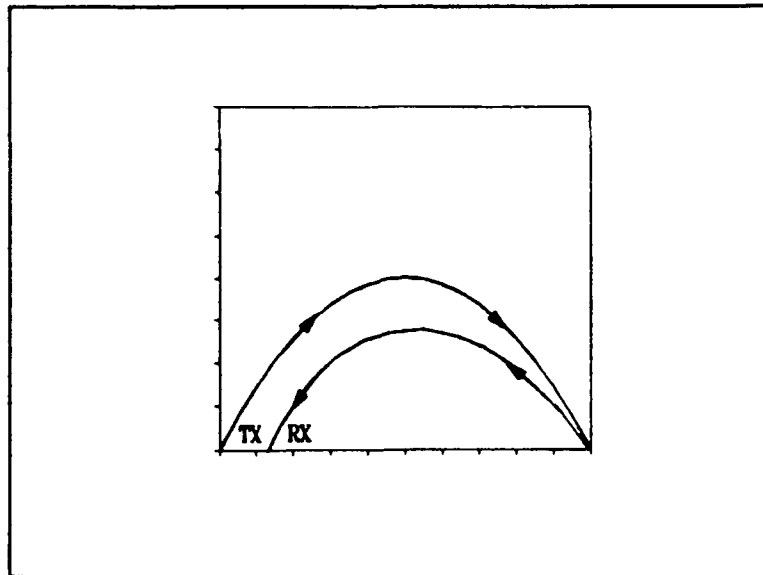


Figure 7 - Oblique Bistatic Pulse Sounding

Figure 8 - Oblique Backscatter Pulse Sounding



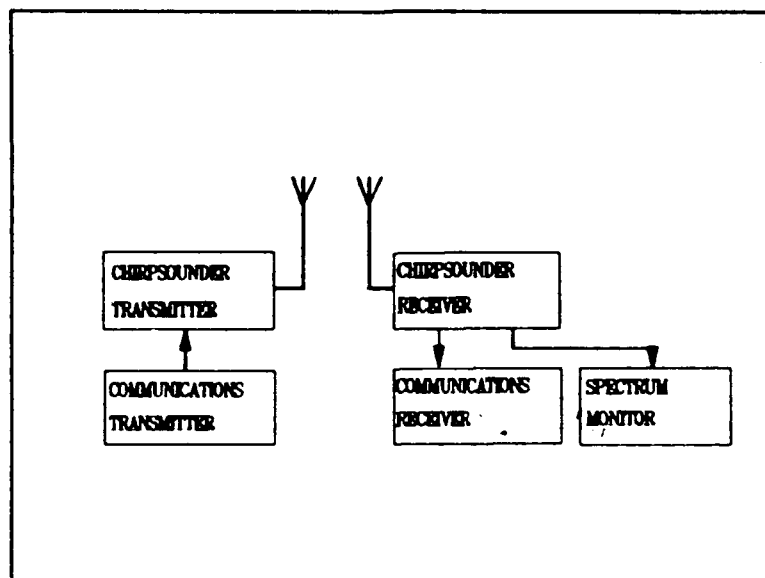Figure 9 - Block Diagram of Chirpsounding System

# APPENDIX D - GLOSSARY

- Ionosphere ...................... The ionosphere extends from 50 Km to 400 km in altitude. At these distances from the surface, the air is very thin and the pressure is very low: from 2 mm to $10^{-6}$ mm of mercury is a typical range. By contrast, sea level pressure is 760 mm. At such low pressures as those at the upper levels, the atoms of atmospheric gases are readily ionized by the actinic ultraviolet (UV) light from sunlight. These ionized gases expel electrons which can reflect radio waves at certain frequencies corresponding to their mean free paths of travel before collision with un-ionized atoms or molecules [Ref. 14].

- Skywaves and groundwaves ......... Radiated radio waves are propagated in two main modes, by groundwaves which hug the surface of the ground in the troposphere and follow the earth's curvature in this manner, and by skywaves which are propagated in straight lines until intercepted by the ionosphere, which reacts in a quasi-optical manner (like a prism) by bending their paths continuously toward the earth, up to a limiting frequency. This bending results in reflection back to the ground [Ref. 14].

- Ionospheric layers ............... The ionized region consists of mixture of free electrons and both positive and negative ions distributed in a plasma-like medium at very low pressure. Only the free electrons can move with sufficient velocity to interact with high-frequency radio waves. Although the ionization extends continuously through the ionosphere, there are heights at which the free electron density reaches a maximum density. These regions of maximum density are called layers (D,E,F1,F2) [Ref. 14].

- Ionization density ............... The density of ionization or concentration of free electrons is quite low in the D-layer. It is the lowest in height and is protected from UV radiation by the higher E-layer and F-layer. However, it tends to be ionized by solar X-rays which penetrate further than the UV layer and make this layer a mixture of electrons and un-ionized molecules. As the latter are relatively dense, they absorb most of the

50

electrons excited by radio waves, and thus remove energy from the signal. This attenuation occurs mainly during the sunlight hours. The E-layer has adequate electron mean free path length to resonate with HF waves, and therefore acts as a reflecting layer. However, it is very thin in height and at night may lose most of its ionization by recombination of ions and electrons. The F1-layer is part of the total F-layer complex. It, like the E-layer, is predominantly a daytime phenomenon. the F1-layer is lower than the F2-layer, but merges with it to some degree at night. The F2-layer is the highest known layer that reflects radio waves. It is highly ionized and remains at reduced density, even at nighttime. Its height is quite variable, reaching the greatest altitudes around local noon [Ref. 14].

• Es ............................... Sporadic E is the thin layer of enhanced ionization confined to the E region (100-110 Km) and is thought to be a result of an enhanced concentration of ions caused by wind shears in that region [Ref. 6].

• Spread F ......................... Spread F is caused by the scattering of the signal from irregularities embedded in the i,nosphere both in depth and away from the zenith. The echo pulse reflected from the F2 layer has a much longer duration than the transmitted pulse. The echoes obtained from that layer by vertical sounding become diffuse and of indefinite height. The effect in the F2 layer soon after local sunset, and which appears to last for a few hours thereafter in a region near the earth's magnetic equator is known as "equatorial spread F" [Ref. 16].

• Tilts ............................ Ionospheric tilts refer to generally large-scale horizontal gradients in the electron density, such that contours of constant electron density are no longer parallel to the earth's surface [Ref. 6].

• TIDs ............................. Traveling ionospheric disturbances are essentially an ionospheric manifestation of an entire spectrum (not necessarily continuous) of waves propagating through the atmosphere [Ref. 6].

• Vertical sounding ................ Transmission of a HF wave vertically to the ionosphere is a means of determining its height and frequency-reflecting characteristics. The transit time delay is a function of the height to the maximum intensity layer. The upper

frequency limit is a measure of the degree of ionization [Ref. 14].

- Oblique sounding ................. In oblique sounding, the angle of incidence of the transmitted radio wave is less than 90 degrees. Thus, the point of return to ground is remote from the transmitter. This wave can then be reflected alternately between the earth and the ionosphere several times. Through variations in the ionosphere and/or multi-angle radiation from the antenna, many reflection paths can be taken by the reflected waves. It is also possible for individual reflections from the E-layer and F-layer to interact. These can, and often do, exist simultaneously, causing multisignal reflection from a single transmitter at a remote receiving point. The oblique type of sounding is valuable for the investigation of propagation paths over any practical path using the ionosphere [Ref. 14].

- Virtual height ................... Normally designated $h'$, the virtual height is the height at which a signal transmitted toward the ionosphere appears to be reflected. It is also the height obtained by vertical incidence sounders, since the time delay of the actual path of the signal is nearly the same as the apparent path of the signal, provided that the ionosphere is treated as a plane mirror at the apex of the apparent path. As the frequency of a vertically incident transmitted signal is increased, the measured virtual height of the signal's reflection increases. Although the actual speed in the ionosphere is less than in free space; the height is calculated as if the medium were free space, hence the adjective "virtual." [Ref. 14]

- hmF2, hmF1, and hmE .............. The height of the maximum electron density in the F2 and F1 layers and the E-region respectively.

- Critical frequency ............... It is the highest frequency which is reflected back to ground during vertical sounding. At oblique angles of incidence, with longer paths traversed through the ionosphere, higher frequencies can be reflected back to earth, and calculated as a product of the critical frequency with the sine of the oblique angle of incidence [Ref. 14].

- Maximum usable frequency (MUF) ... The maximum frequency that can be used for long range communications (>3000 km) can be higher than the critical frequency of vertical sounding. This maximum usable frequency for oblique incidence transmission is calculated as the product of the

52

critical frequency and the secant of the oblique angle of incidence (secant law). This formula assumes a flat earth and a similarly flat F-layer. The curvature of the earth introduces serious errors beyond a few kilometers. Frequencies between the highest and lowest usable limits will be transmitted and received. However, many frequencies in this band are subject to multiple reflections which degrade the quality of reception. The shortest distance at which any frequency can be received by reflections is the "skip" distance. The skywave signals cannot be received at shorter distances than the "skip" distance [Ref. 14].

• Multipath interference .......... When the frequency of transmission is appreciably less than the MUF, the signals are received by several propagation paths having different delay times. These time differences result in distortion of phase of the signal modulation, which can be severe in the case of navigational signals, and cause selective fading of side frequencies in the modulation sidebands. Since the propagation paths are very sensitive to geometrical variations of the reflection angles, turbulence in the ionosphere, which is common, causes either rapid or slow variations of flutter-fading through changing delay times. While frequencies near the MUF are less susceptible to multipath transmission, they are subject to flutter-fading due to temporary variations in the locally ionized regions [Ref. 14].

• Ordinary and Extraordinary Rays .. The permanent magnetic field of the Earth makes the ionized gas of the ionosphere an anisotropic medium (different properties in different directions). When a linearly polarized wave is propagated in a arbitrary direction relative to the direction of the magnetic field of the earth, the wave is split into two elliptic rays, the ordinary (O) and the extraordinary (E) rays. The longitudinal electric field components of both the E and O rays are in phase with the transverse component, oriented in the direction of the magnetic field of the earth. These rays are propagated with different velocities and paths, and the major axes of the ellipses of polarization are at the right angles to each other, with the resultant vectors rotating in opposite directions [Ref. 17] .

• Gyro-frequency ................... The rotation of the electrons under the effect of the terrestrial magnetic field exhibits resonance characteristics. This is why it is sometimes referred to as gyromagnetic resonance, and the respective frequency is called the gyro-frequency. The average value of the constant magnetic field of the earth,

$H_o$, is 40 A/m and gives 1.4 MHz as the gyro-frequency. It may be expected that waves at a frequency of about 1.4 MHz will experience increased attenuation in the ionosphere due to collision losses [Ref. 17].

- foF2, foF1, and foE .............. The critical frequency of the ordinary wave for the F2 and F1 layers and the E region, respectively [Ref. 18].

- M(n)X ............................ The maximum usable factor for a path of "n" kilometers for transmission by the "X" layer. For example, M(3000)F2 represents the maximum usable factor for a path of 3000 km for transmission by the F2 layer [Ref. 18].

- Geomagnetic Latitude ............. The boundaries between the low, middle, and high latitudes are not fixed, but vary with local time, season of year, and solar cycle. So, the "low latitude" can be viewed as extending from between +/- 30° geomagnetic latitude, the "high latitude" greater than 60° geomagnetic latitude, and "middle latitude" as the geomagnetic latitudes between 30° and 60°. Because the geomagnetic and geographic poles do not coincide, there are substantial differences between the geographic and geomagnetic latitudes, particularly in the Americas and throughout Asia.

- Covariance ...................... Covariance measures how strongly two random variables X and Y are related to one another [Ref. 4].

# APPENDIX E - IONOSPHERIC DATA RESEARCH

In the region near the earth's magnetic equator, several magnetic and ionospheric phenomena occur that appear to be peculiar to that region. Evidently, much investigation must be done before these occurrences become fully explained.

"The Condor Equatorial Spread F Campaign," published at the *Journal of Geophysical Research*, Vol. 91, No A5, (May 1, 1986), summarizes the main results of many experiments designed to study the South American equatorial F region [Ref. 19].

Based on that publication the following agencies, were contacted in June, 1990 to suggest a source of vertical incidence ionosonde data or incoherent scatter measurements which could be use to establish the normal vs. tilted ionospheric profiles in that region. Unfortunately, none of these requests produced positive results.

- Air Force Cambridge Research Laboratories, Bedford, Massachusetts

- Center for Atmospheric and Space Sciences, Utah State University, Logan, Utah

- Emmanuel College, University of Massachusetts, Boston, Massachusetts

- Instituto Geofisico del Peru, Lima, Peru[1]

- Ionospheric Physics Division, Air Force Geophysics Laboratory, Hanscon Air Force Base, Massachusetts

- Los Alamos National Laboratory, Los Alamos, New Mexico

- National Space Research Institute (INPE), Sao Jose dos Campos, SP, Brazil [2]

- School of Electrical Engineering, Cornell University, Ithaca, New York

- Space Physics Research Laboratory, University of Michigan, Ann Arbor, Michigan

- The University of Texas at Dallas, Dallas, Texas

---

[1] Dr. Ronald F. Woodman, Director of the "Instituto Geofisico Del Peru" reported that data from "Radio Observatorio de Jicamarca" are single station (no tilt information).

[2] INPE was recommended by Mr Jorgen Buchau from the Ionospheric Physics Division, Hanscon Air Force Base, Massachusetts.

# LIST OF REFERENCES

1. McNamara, L.F., *Ionospheric Limitations to the Accuracy of SSL Estimates of HF Transmitter Locations*, AGARD SYMPOSIUM - Munich, 1988.

2. Heaps, M.G., and others, *High Frequency Position Location: An Assessment of Limitations and Potential Improvements*, Atmospheric Sciences Laboratory, US Army, 1981.

3. Gautier, T.N., *The Use of Correlation Coefficients in the Estimation of the Current Value of an Ionospheric Parameter*, NBS Report 7696, 1962.

4. Devore, J.L., *Probability and Statistics for Engineering and the Sciences*, Brooks/Cole Publishing Company, 1987.

5. Weiss, N.A., and Hasset, M.J., *Introductory Statistics*, 2nd Edition, Addison-Wesley Publishing Company, 1987.

6. Heaps, M.G., *Accounting for Ionospheric and Irregularity in High Frequency Direction Finding*, Atmospheric Sciences Laboratory, U.S. Army, 1982.

7. Rush, C. M., and Gibbs, J., *Predicting the Day-to-Day Variability of the Mid-Latitude Ionosphere for Application to HF Propagation Predictions*, AFCRL Technical Report 73-0335, 1973.

8. Rush, C. M., *HF Propagation: What We Know and What We Need to Know*, Second International Conference on Antennas and Propagation, Part 2 -Propagation, Publication No 195, Electronics Division of the Institution of Electrical Engineers, 1981.

9. Fenwick, R.B., *Backscatter-Sounding Study of Coverage of VOA Broadcasts to Brazil*, Radioscience Laboratory, Stanford University, Technical Report No. IA-4, 1967.

10. Bennington, T.W., *Equatorial Ionospheric Effects*, Wireless World, October 1960.

11. Zacharisen, D.H., *Some Applications of the Theory of using Observations at Ionosphere Stations to Estimate Current Values of Ionospheric Characteristics at other Locations*, NBS Report 8226, 1964.

12. Gething, P.J.D., *Radio Direction Finding and the Resolution of Multicomponent Wave-fields*, Peter Peregrinus Ltd., 1989.

13. Grossman, S.I., *Multivariable Calculus, Linear Algebra, and Differential Equations*, Harcourt Brace Jovanovich Inc., 1986.

14. Moision, W. K., Hildebrand, V. E., Rose, R. B., *Analysis of Predicted Maximum Usable Frequency and Maximum Observed Frequency over a Guam-To-Australia Transequatorial Path*, Naval Weapons Center, 1970.

15. Maslin, N., *HF Communications - A Systems Approach*, Plenum Press, 1987.

16. Davies, K., *Ionospheric Radio Propagation*, Dover Publications Inc., 1966.

17. Dolukhanov, M., *Propagation of Radio Waves*, Mir Publishers, 1971.

18. Piggott, W.R., and Rawer, K., *URSI Handbook of Ionogram Interpretation and Reduction of the World Wide Sounding Committee*, Elsevier Publishing Company, 1961.

19. Kelley, M.C., and others, *The Condor Equatorial Spread F Campaign: Overview and Results of the Large-Scale Measurements*, Journal of Geophysical Research, Vol. 91, No. A5, May 1, 1986.

# INITIAL DISTRIBUTION LIST

1. Defense Technical Information Center                                   2
   Cameron Station
   Alexandria, Virginia 22304-6145

2. Library, Code 52                                                       2
   Naval Postgraduate School
   Monterey, California 93943-5002

3. Chairman, Electronic Warfare Academic Group                           1
   Code EW
   Naval Postgraduate School
   Monterey, California 93943

4. Professor R. W. Adler                                                  3
   Code EC/Ab
   Department of Electrical and Computer Engineering
   Naval Postgraduate School
   Monterey, California 93943

5. Professor S. Jauregui, Jr.                                            1
   Code EC/Ja
   Department of Electrical and Computer Engineering
   Naval Postgraduate School
   Monterey, California 93943

6. Estado Maior do Exército (5a Sub/Ch)                                  1
   Att. TC Carlos Augusto Teixeira Filho
   Quartel General do Exército
   Setor Militar Urbano
   Brasília, DF 70000
   Brazil

7. Commander Naval Space and Naval Warfare Systems Cmd.                  1
   Attention: LCDR E. R. Arbogast
   PMW-143
   Washington, D.C. 20363

8. Commander Naval Security Group Command                               1
   Naval Security Group
   Attention: G-82
   Nebraska Ave.
   Washington, D.C. 20390